



## Thermal conductivity of symmetrically strained Si/Ge superlattices

THEODORIAN BORCA-TASCIUC<sup>†</sup>, WEILI LIU<sup>†</sup>, JIANLIN LIU<sup>‡</sup>, TAOFANG ZENG<sup>†</sup>,  
DAVID W. SONG<sup>†</sup>, CAROLINE D. MOORE<sup>§</sup>, GANG CHEN<sup>†\*</sup>, KANG L. WANG<sup>‡</sup>,  
MARK S. GOORSKY<sup>§</sup>

<sup>†</sup>*Mechanical and Aerospace Engineering Department*, <sup>‡</sup>*Department of Electrical Engineering*, <sup>§</sup>*Materials Science & Engineering Department, University of California, Los Angeles, CA 90095-1597, USA*

TAMARA RADETIC<sup>¶</sup>, RONALD GRONSKY<sup>||</sup>

<sup>¶</sup>*Materials Science Division, Lawrence Berkeley National Laboratory, Berkeley, CA 94720, USA*

<sup>||</sup>*Department of Materials Science and Mineral Engineering, University of California, Berkeley, CA 94720, USA*

TAKAAKI KOGA<sup>\*\*</sup>, MILDRED S. DRESSELHAUS<sup>††, ‡‡</sup>

<sup>\*\*</sup>*Division of Engineering and Applied Sciences, Harvard University, Cambridge, MA 02138, USA*

<sup>††</sup>*Department of Physics*, <sup>‡‡</sup>*Department of Electrical Engineering and Computer Science, Massachusetts Institute of Technology, Cambridge, MA 02139, USA*

(Received 14 April 2000)

---

This paper reports temperature-dependent thermal conductivity measurements in the cross-plane direction of symmetrically strained Si/Ge superlattices, and the effect of doping, period thickness and dislocations on the thermal conductivity reduction of Si/Ge superlattices. The Si/Ge superlattices are grown by molecular beam epitaxy on silicon and silicon-on-insulator substrates with a graded buffer layer. A differential  $3\omega$  method is used to measure the thermal conductivity of the buffer and the superlattices between 80 and 300 K. The thermal conductivity measurement is carried out in conjunction with X-ray and TEM sample characterization. The measured thermal conductivity values of the superlattices are lower than those of their equivalent composition bulk alloys.

© 2000 Academic Press

**Key words:** thermal conductivity, superlattice, thermoelectrics phonon engineering.

---

### 1. Introduction

Understanding the thermal conductivity and heat transfer processes in thin films and superlattice structures is critical for the development of microelectronic and optoelectronic devices [1] and low-dimensional thermoelectric and thermionic devices [2]. Experimental results on the thermal conductivity of superlattices have been reported in recent years for several materials systems, including GaAs/AlAs [3–5], GaAs/AlGaAs [6],

\*To whom correspondence should be addressed. E-mail: [gchen@seas.ucla.edu](mailto:gchen@seas.ucla.edu)

Si/SiGe [7], Si/Ge [8–10] and Bi<sub>2</sub>Te<sub>3</sub>/Sb<sub>2</sub>Te<sub>3</sub> [11–13]. These studies demonstrate that the thermal conductivity of a superlattice could be much lower than that estimated from the bulk values of its constituent materials [3], and even smaller than the thermal conductivity values of the equivalent composition alloys. In order to explain these findings, models for the thermal conductivity of superlattices, based on minigap scattering [14], the Boltzmann transport equation [15, 16], and phonon group velocity reduction [17–19], have been developed. Furthermore, the models suggest the possibility of controlling the thermal conductivity of superlattice structures through phonon engineering [20, 21].

One of the most significant reductions in the thermal conductivity of superlattices has been reported for the Si/Ge superlattice system [8]. The measured thermal conductivity reduction, coupled with the possible increase of the Seebeck coefficient and electrical conductivity due to quantum confinement effects in these superlattices [22], makes the Si/Ge superlattice system a good candidate for highly efficient thermoelectric energy conversion. Previously reported experimental studies on Si/Ge superlattices [8] were based on samples grown by metal-organic chemical-vapor deposition (MOCVD) on GaAs substrates with Ge buffers. The use of un-symmetrically strained Si and Ge layers in the superlattice films leads to high density of threading dislocations, making the interpretation and modeling of the experimental results difficult.

This paper uses symmetrically strained Si/Ge superlattices and reports temperature-dependent thermal conductivity measurements in the cross-plane direction of symmetrically strained, molecular-beam-epitaxy (MBE) grown Si/Ge superlattices and the effect of doping, period thickness and dislocations on the thermal conductivity reduction in these superlattices. The Si layer and Ge layer in the superlattice period have the same thickness, ranging from 22–70 Å (for each layer) for different samples. The effect of doping is evaluated for several 40 Å period, symmetrically strained superlattices, p-type and n-type doped with carrier concentrations between  $1 \times 10^{18} \text{ cm}^{-3}$  and  $2 \times 10^{19} \text{ cm}^{-3}$ . Thermal conductivity measurements are performed using the  $3\omega$  method [23]. In this technique the temperature drop across the superlattice film is experimentally determined and used to estimate the thermal conductivity of the film. Transmission electron microscopy (TEM) and X-ray characterization measurements are employed to study the quality of the superlattices. Thermal conductivity measurements have been carried out for the Si/Ge superlattices in the temperature range from 80 K to room temperature. The experimental data demonstrate a strong reduction in the thermal conductivity of the Si/Ge symmetrically strained superlattices.

## 2. Samples and experiments

The Si/Ge superlattices are grown by MBE on Si100 and SOI wafers and the layer configuration for each sample is summarized in Table 1. The influence of the periodicity on the superlattice thermal conductivity is studied for the superlattices JL155, JL156 and JL157, which have, respectively, 140, 44 and 90 Å for each period and are grown without doping on Si substrates. The effect of doping concentration is studied for uniformly doped n-type (Sb doped) and p-type (B doped) 40 Å period superlattices grown on SOI substrates. The SOI substrates are selected in order to facilitate thermoelectric measurements presented elsewhere [24]. The doping concentrations are  $n^+ \sim 1\text{--}2 \times 10^{18}$  for JL199,  $n^+ \sim 4\text{--}5 \times 10^{18}$  for JL197,  $n^+ \sim 2 \times 10^{19}$  for JL194 and  $p^+ \sim 1\text{--}2 \times 10^{19}$  for JL196.

In order to grow equal layer thickness Si/Ge superlattices, it is necessary to prepare a buffer layer with a lattice constant on the top surface equal to the average lattice constant of Si and Ge. The superlattices grown on this buffer have a symmetric, ‘zero’ strain configuration over one period, because the strain in the Ge layer is compressive and the strain in the Si layer is of equal value and opposite sign (tensile). Detailed growth and configuration of the buffer layer are described in Ref. [25]. The growth starts with a 1000 Å Si buffer. One monolayer of Sb surfactant is deposited, followed by the growth of the continuously graded Si<sub>1-x</sub>Ge<sub>x</sub> layer with the Ge mole fraction beginning from 0 to 0.5. The thickness of the continuously graded layer is 2 μm for samples JL155, JL156 and JL157 and 1 μm for samples JL194, JL196, JL197 and JL199. The buffer growth ends with the deposition of 0.3 μm Si<sub>0.5</sub>Ge<sub>0.5</sub>. The growth temperature of the superlattice layers is 510 °C

**Table 1:** Sample configurations.

Sample	One period	Periods	Doping ( $\text{cm}^{-3}$ )	Buffer
JL155	Si(70 Å)/Ge(70 Å)	33	—	2 $\mu\text{m}$ continuous graded Si $\rightarrow$ $\text{Si}_{0.5}\text{Ge}_{0.5}$ + 0.3 $\mu\text{m}$ $\text{Si}_{0.5}\text{Ge}_{0.5}$
JL156	Si(22 Å)/Ge(22 Å)	100	—	same as JL155
JL157	Si(45 Å)/Ge(45 Å)	50	—	same as JL155
JL194	Si(20 Å)/Ge(20 Å)	100	$n^+ \sim 2 \times 10^{19}$	1 $\mu\text{m}$ continuous graded Si $\rightarrow$ $\text{Si}_{0.5}\text{Ge}_{0.5}$ + 0.3 $\mu\text{m}$ $\text{Si}_{0.5}\text{Ge}_{0.5}$
JL196	Si(20 Å)/Ge(20 Å)	100	$p^+ \sim 1-2 \times 10^{19}$	same as JL194
JL197	Si(20 Å)/Ge(20 Å)	100	$n^+ \sim 4-5 \times 10^{18}$	same as JL194
JL199	Si(20 Å)/Ge(20 Å)	100	$n^+ \sim 1-2 \times 10^{18}$	same as JL194

for the undoped samples and 380 °C for the doped samples. Dopant activation for the doped superlattices is achieved by a 10 min annealing step at 580 °C.

A differential  $3\omega$  method is employed to perform the cross-plane thermal conductivity measurements on the Si/Ge superlattices. In the  $3\omega$  method [23], a metal wire is deposited onto the film to act as both a heater and a temperature sensor. Since the superlattice film is semiconducting, the metal wire must be insulated from the film to avoid current leakage. The electrical insulation is provided by  $\sim 100$  nm  $\text{SiN}_x$  film deposited by plasma enhanced chemical-vapor deposition (PECVD) at 275 °C onto the samples. In order to determine the thermal conductivity of the Si/Ge superlattice film, the temperature drop across the superlattice is determined. This temperature drop is experimentally measured by a differential technique using a series of samples, as illustrated in Fig. 1. The differential  $3\omega$  thermal conductivity characterization of the superlattice requires deposition of wires on three different samples, including a substrate, a buffer grown on the substrate and a superlattice grown on the identical buffer. The insulation layer and the metallic heaters/temperature sensors with wire widths between 2 and 50  $\mu\text{m}$  are processed for all the samples during the same process flow. For a given wire width, the temperature rise at a given frequency and identical power input is recorded for the substrate, buffer and superlattice samples. The measured temperature difference between the substrate sample and the buffer sample is used to determine the thermal conductivity of the buffer. Furthermore, the measured temperature difference between the buffer sample and the superlattice sample is used to determine the thermal conductivity of the superlattice. Both the in-plane and the cross-plane thermal conductivity of the films can be determined if the experiment is carried out for different heater width/film thickness aspect ratios and a two-dimensional heat conduction model is used to fit the experimental temperature drop across the film [7, 26]. However, a simpler one-dimensional heat conduction model can be used to determine the cross-plane thermal conductivity of the film if the width of the heater is much larger than the film thickness, and if the film thermal conductivity is much smaller than the substrate thermal conductivity [26]. In this work, 30  $\mu\text{m}$  width heaters are used to measure the temperature drop across  $\sim 0.5$   $\mu\text{m}$  thick superlattice films. The heater-width/superlattice-thickness aspect ratio is  $\sim 60$ , and the ratio between the superlattice thermal conductivity and substrate thermal conductivity is at most  $\sim 0.033$ . Under the above conditions, one-dimensional heat conduction modeling for the heat transport across an anisotropic film yields an error of  $< 2\%$  for its thermal conductivity, as long as the film anisotropy of thermal conductivity is smaller than five [26]. However, the measured Si/Ge superlattices are grown on relatively thick 1.3–2.3  $\mu\text{m}$  buffer layers and the film anisotropy is unknown. Due to the heat spreading effect in the buffer layers, the one-dimensional heat conduction approximation generates large errors in the measured thermal conductivity of the buffer and

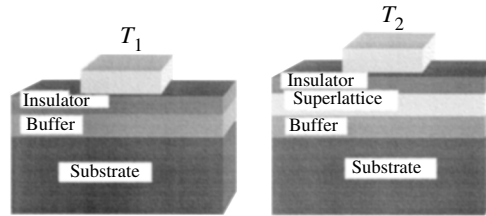


Fig. 1. Differential  $3\omega$  method.

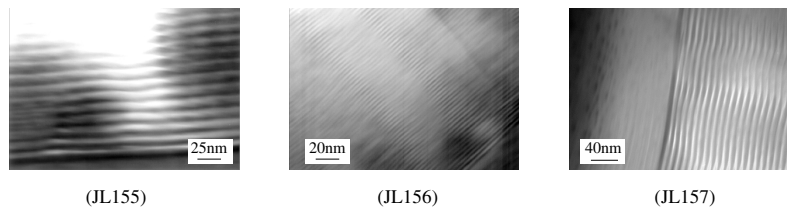


Fig. 2. TEM micrographs of undoped Si/Ge superlattices.

superlattice films. Therefore, a two-dimensional, multilayer, anisotropic heat conduction model was used to back up the cross-plane thermal conductivities of the Si/Ge superlattices reported in this work.

The temperature-dependent thermal conductivity measurements were carried out in a cryostat in the temperature range from 80 K to room temperature. The temperature in the chamber was adjusted to the desired temperature by a temperature controller. During the  $3\omega$  measurements, the ambient temperature variations in the cryogenic chamber were within 0.1 K. The calibration of the temperature coefficient of resistance (TCR) of the metallic wire was carried out during the slow warm-up of the cryostat. The  $3\omega$  voltage was measured by a lock-in amplifier. A computer was used for automatic data acquisition and control.

### 3. Experimental results and discussion

X-ray diffraction and transmission electron microscopy (TEM) were employed to evaluate the quality and periodicity of the JL155, JL156 and JL157 Si/Ge superlattices. The above-mentioned samples show good X-ray diffraction peaks and the electron diffraction patterns reveal satellite spots due to the superlattice periodicity. These results confirm the quality and periodicity of the JL155, JL156 and JL157 superlattices. Furthermore, cross-sectional transmission electron micrographs of the Si/Ge superlattices (Fig. 2) verify the periodicities of the superlattices and the morphologies of both the buffer layers and the superlattice films.

Figure 3 shows the temperature dependent cross-plane thermal conductivity of the symmetrically strained Si/Ge superlattices JL155, JL156 and JL157. The experimental results indicate a strong reduction in the thermal conductivity of the symmetrically strained Si/Ge superlattices relative to the Si/Ge alloy film. The thermal conductivity values vary from 2.9–4.0  $\text{W m}^{-1} \text{K}^{-1}$  at room temperature to 2.6–3.5  $\text{W m}^{-1} \text{K}^{-1}$  at 83 K. As a general trend, the thermal conductivity of the superlattices decreases with decreasing temperature. The thermal conductivity values of the Si/Ge superlattices measured in this work are slightly higher than the values measured by Lee *et al.* [8] on Si/Ge superlattices with comparable superlattice periods, but still lower than the thermal conductivity of the  $\text{Si}_{0.5}\text{Ge}_{0.5}$  alloy samples. It should be noted that the superlattice samples reported in Ref. [8] were not symmetrically strained, were grown on different buffers with the MOCVD method and were doped with carrier concentrations between  $3\text{--}20 \times 10^{18} \text{ cm}^{-3}$ . Therefore, the lower thermal

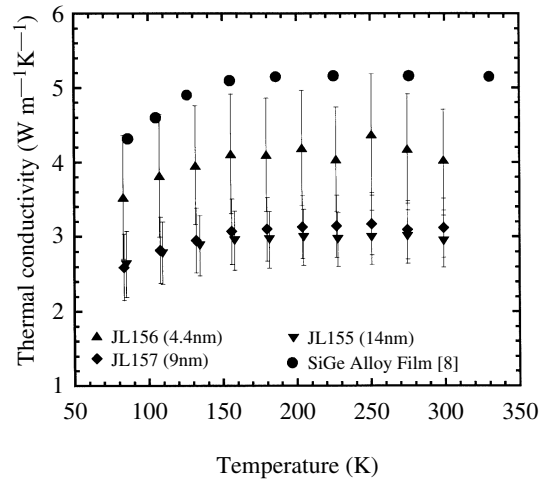
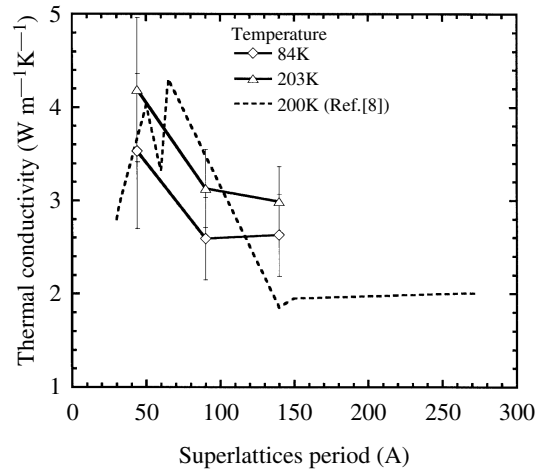


Fig. 3. Temperature dependence of the thermal conductivity of undoped Si/Ge superlattices.

conductivity values in Lee's [8] samples could be due to additional phonon scattering by dopants and dislocations arising from the strained relaxation in the un-symmetrically strained film. The error bars in Fig. 3 represent the experimental uncertainty of the thermal conductivity. If the thermal conductivity anisotropy of the superlattice and buffer films is smaller than four (i.e. the cross-plane thermal conductivity is no more than four times smaller than the in-plane thermal conductivity) or if the buffer anisotropy is larger than the anisotropy of the superlattice, then the estimated values of the cross-plane thermal conductivity of the superlattices reported in this work are within the experimental uncertainties shown in Fig. 3. Narrower heaters must be used in order to measure more accurately the in-plane thermal conductivity of the superlattices.

The superlattice period thickness dependence of the thermal conductivity is shown in Fig. 4. The results in Ref. [8] are also plotted for comparison. Venkatasubramanian and Colpits [9] suggested that the dip in the data of Lee *et al.* [8] is physical rather than an experimental variation and provided in-plane thermal conductivity data with a large dip in the thermal conductivity at around a 65 Å period thickness. The current sample series does not have enough data points to confirm their observations. Our cross-plane thermal conductivity data show a decreasing trend as the period thickness increases, and a relatively small dependence on superlattice period for periods between 90 and 140. Lee *et al.* [8] suggested that the drop in thermal conductivity of the Si/Ge superlattices at larger periods is due to the formation of dislocations in the studied samples. The modeling of Chen and Neagu [15] indicates that the needed dislocation density is  $\sim 10^{11}$ – $10^{12}$  cm<sup>-2</sup>. Cross-sectional TEM micrographs of the JL155, JL156 and JL157 superlattices show threading dislocations propagating from the top surface of the buffer layer into the superlattice films. However, quantitative estimations of the dislocation densities using a Schimmel defect etch and counting the etch pits with a Nomarski interference microscope yields the same range of dislocation densities in all three samples in Fig. 3. The dislocation density in the above superlattices is estimated to be  $\sim 1.5 \times 10^4$  lines cm<sup>-2</sup> and is equal to the dislocation density on the top surface of the buffer [25]. Therefore, a different mechanism, other than threading dislocations, must be responsible for the reduction in thermal conductivity of the larger period Si/Ge superlattices. One possible reason could be the increasing residual stress within the layers of larger period Si/Ge superlattices.

In order to study the effect of carrier type and concentration on the thermal conductivity reduction, superlattices JL194, JL196, JL197 and JL199 were grown on SOI substrates with a 1.3 μm continuously graded SiGe buffer. The reason for the use of SOI substrates is to facilitate the electrical conductivity measure-



**Fig. 4.** Thermal conductivity of the symmetrically strained Si/Ge superlattices as a function of period thickness, at two temperatures and in comparison with results in Ref. [8].

ments [27]. Due to the smaller buffer layer thickness, the density of threading dislocations in the top surface of the buffer layer is  $\sim 1.5 \times 10^8$  lines  $\text{cm}^{-2}$ , four orders of magnitude larger than the density of threading dislocations in the JL155, JL156 and JL157 superlattices.

Figure 5 shows the temperature dependent thermal conductivity of several 40 Å period Si/Ge superlattices with different doping concentrations. These doped superlattices have smaller thermal conductivity values than the 44 Å period undoped JL156 superlattice shown in Fig. 3, possibly indicating the influence of higher dislocation densities and doping on the thermal conductivity reduction. The thermal conductivity of a p-type superlattice (JL196) is larger than the thermal conductivity of an n-type superlattice doped with the same dopant concentration (JL194). The n-type samples doped at higher carrier concentrations have higher thermal conductivity values. This behavior is opposite to the doping effect reported for bulk silicon [28], where the heat conduction is impeded by higher dopant concentrations. In bulk silicon, the lattice thermal conductivity reduction due to the scattering by dopant ions is more than the increase of the electronic thermal conductivity. In superlattices, due to the already low phonon thermal conductivity, it is possible that the electronic thermal conductivity makes a large contribution to the total thermal conductivity. Currently, we do not have cross-plane electrical conductivity measurements for these superlattices, so we used the measured in-plane electrical conductivity and the calculated Lorentz number to estimate the electronic thermal conductivity based on the Wiedeman–Franz law. The calculated relative electronic contribution at 300 K is  $\sim 10\%$  of the total thermal conductivity for JL194,  $\sim 6\%$  for JL197 and  $\sim 5\%$  for JL199. At 80 K the relative electronic contribution to the total thermal conductivity is  $\sim 5\%$  for JL194,  $\sim 2\%$  for JL197 and  $< 2\%$  for JL199. These preliminary results indicate an increase in the relative electronic contribution to the total thermal conductivity at higher doping concentrations but do not quantitatively explain the thermal conductivity trends shown in Fig. 5. Cross-plane electrical conductivity measurements are necessary in order to fully understand the effect of doping on the thermal conductivity of strained Si/Ge superlattices.

#### 4. Conclusion

This work presents experimental results on the temperature dependent cross-plane thermal conductivity of symmetrically strained Si/Ge superlattices grown by MBE on graded buffers, for several superlattices with periodicities from 40–140 Å. The measured thermal conductivity values for the undoped samples are

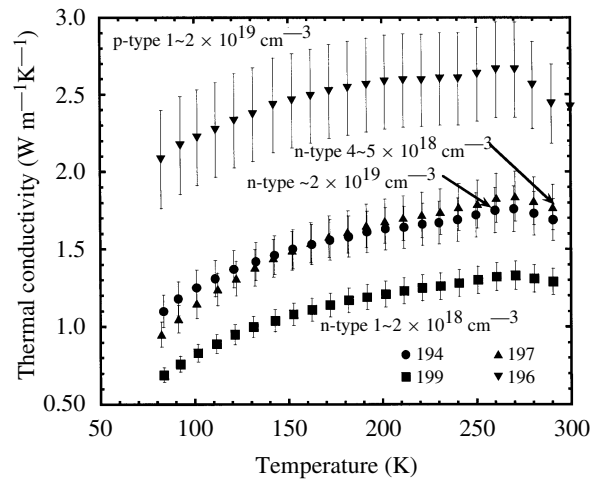


Fig. 5. Temperature dependence of the thermal conductivity of several p-type and n-type doped Si(20 Å)/Ge(20 Å) superlattices.

lower than those of the corresponding bulk alloy, but higher than those reported in the literature for comparable thickness, doped, asymmetric superlattices grown by MOCVD on Ge buffers. The doped superlattices characterized in this work have larger dislocation densities than the undoped samples and lower thermal conductivity values. The thickness dependence of the studied samples and the doping effect shows a complex behavior that has yet to be fully understood.

*Acknowledgements*—G. Chen thanks Dr A. C. Ehrlich for helpful discussions. This work is supported by a DOD MURI grant on thermoelectrics (N00014-97-1-0516). The authors would like to express gratitude to the National Center for Electron Microscopy (NCEM) at Lawrence Berkeley National Laboratory (LBNL) for providing TEM facilities.

## References

- [1] G. Chen, Heat transfer in micro- and nanoscale photonic devices, in *Annual Review of Heat Transfer*, edited by C. -L. Tien (Begel, 1996) Vol. 7, p. 1.
- [2] G. Chen, S. Volz, T. Borca-Tasciuc, T. Zeng, D. Song, K. L. Wang, and M. S. Dresselhaus, Thermal conductivity and photon engineering in low dimensional structures, *Mater. Res. Soc.* **545**, 357 (1998).
- [3] T. Yao, *Appl. Phys. Lett.* **51**, 1798 (1987).
- [4] X. Y. Yu, G. Chen, A. Verma, and J. S. Smith, *Appl. Phys. Lett.* **67**, 3554 (1995).
- [5] W. S. Capinski and H. J. Maris, *Physica* **B219**, 699 (1996).
- [6] G. Chen, C. L. Tien, X. Wu, and J. S. Smith, *J. Heat Transfer* **116**, 325 (1994).
- [7] G. Chen, S. Q. Zhou, D. J. Yao, C. J. Kim, X. Y. Zheng, J. L. Liu, and K. L. Wang, Heat conduction in alloy-based superlattices, in *Proceedings of the 17th International Thermoelectrics Conference* (IEEE, New York, 1998) p. 202.
- [8] S. M. Lee, D. G. Cahill, and R. Venkatasubramanian, *Appl. Phys. Lett.* **70**, 2957 (1997).
- [9] R. Venkatasubramanian and T. Colpits, Enhancement in figure-of-merit with superlattice structures for thin-film thermoelectrics devices, *Mater. Res. Soc.* **478**, 73 (1997).
- [10] R. Venkatasubramanian, E. Siivola, and T. Colpits, In-plane thermoelectric properties of freestanding Si/Ge superlattice structures, in *Proceedings of the 17th International Thermoelectrics Conference* (IEEE, New York, 1998) p. 191.

- [11] R. Venkatasubramanian, Thin film superlattice and quantum-well structures—a new approach to high-performance thermoelectric materials, *Naval Research Reviews* **58**, 44 (1998).
- [12] I. Yamasaki, R. Yamanaka, M. Mikami, H. Sonobe, Y. Mori, and T. Sasaki, Thermoelectric properties of  $\text{Bi}_2\text{Te}_3/\text{Sb}_2/\text{Te}_3$  superlattice structure, in *Proceedings of the 17th International Thermoelectrics Conference* (IEEE, New York, 1998) p. 210.
- [13] R. Venkatasubramanian, *Phys. Rev.* **B61**, 3091 (2000).
- [14] S. Y. Rev and J. D. Dow, *Phys. Rev.* **B25**, 3750 (1982).
- [15] G. Chen, *J. Heat Transfer* **119**, 220 (1997).
- [16] G. Chen, *Phys. Rev.* **B57**, 14958 (1998).
- [17] P. Hyldgaard and G. D. Mahan, *Phys. Rev.* **B56**, 10754 (1997).
- [18] S. Tamura, Y. Tanaka, and H. J. Maris, *Phys. Rev.* **B60**, 2627 (1999).
- [19] M. V. Simkin and G. D. Mahan, *Phys. Rev. Lett.* **84**, 927 (2000).
- [20] G. Chen, T. Borca-Tasciuc, B. Yang, D. Song, W. L. Liu, T. Zeng, and D. A. Achimov, *Thermal Sci. Eng. (Japan)* **7**, 43 (1999).
- [21] G. Chen, Phonon Heat Conduction in Superlattices and Nanostructures, *Semimet. Semicond.* (in press).
- [22] L. D. Hicks and M. S. Dresselhaus, *Phys. Rev.* **B47**, 12727 (1993).
- [23] D. G. Cahill, *Rev. Sci. Instrum.* **61**, 802 (1990).
- [24] T. Borca-Tasciuc, G. Chen, J. L. Liu, and K. L. Wang, Micro-fabricated test structures for in-plane thermoelectric property characterization of thin films, presented at *2000 MRS Spring Meeting, April 24–28*, San Francisco, CA (2000).
- [25] J. L. Liu, C. D. Moore, G. D. U'Ren, Y. H. Luo, Y. Lu, G. Jin, S. G. Thomas, M. S. Goorsky, and K. L. Wang, *Appl. Phys. Lett.* **75**, 1576 (1999).
- [26] T. Borca-Tasciuc, A. R. Kumar, and G. Chen, Data reduction in the  $3\omega$  method for thin-film thermal conductivity determination, unpublished.
- [27] T. Koga, Concept and applications of carrier pocket engineering to design useful thermoelectric materials using semiconductor superlattices, PhD thesis, Harvard University, (2000).
- [28] G. A. Slack, *J. Appl. Phys.* **35**, 3460 (1964).